IEEE Photonics Journal
An IEEE Photonics Society Publication

Joint Time/Frequency Synchronization and Chromatic Dispersion Estimation With Low Complexity Based on a Superimposed FrFT Training Sequence

Volume 10, Number 5, September 2018

Hexun Jiang
Ming Tang, *Senior Member, IEEE*
Huibin Zhou
Qiong Wu
Yizhao Chen
Songnian Fu
Deming Liu

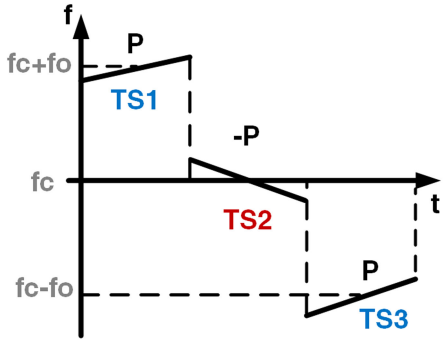

TS structure in the time/frequency domain

DOI: 10.1109/JPHOT.2018.2868745
1943-0655 © 2018 IEEE

Joint Time/Frequency Synchronization and Chromatic Dispersion Estimation With Low Complexity Based on a Superimposed FrFT Training Sequence

Hexun Jiang, Ming Tang, *Senior Member, IEEE*, Huibin Zhou, Qiong Wu, Yizhao Chen, Songnian Fu, and Deming Liu

Wuhan National Laboratory for Optoelectronics and the National Engineering Laboratory for Next Generation Internet Access System, School of Optics and Electronic Information, Huazhong University of Science and Technology, Wuhan 430074, China

DOI:10.1109/JPHOT.2018.2868745

Manuscript received July 23, 2018; revised August 27, 2018; accepted August 31, 2018. Date of current version September 18, 2018. This work was supported in part by the National Natural Science Foundation of China under Grant 61331010 and Grant 61722108; and in part by the Fundamental Research Funds for the Central Universities under Grant HUST 2018KFYXKJC023. Corresponding author: Ming Tang (e-mail: tangming@mail.hust.edu.cn).

Abstract: We design a new kind of fractional Fourier transform superimposed training sequence (TS) to simultaneously estimate linear distortions including chromatic dispersion (CD), timing offset (TO), and frequency offset (FO), etc. Without sacrificing additional spectrum efficiency, the scheme can reduce the computational complexity sharply compared to a regular estimation method. The feasibility of the proposed scheme is verified by simulations of 28 GBaud dual polarization quadrature phase-shift keying (DP-QSPK) and 16-ary quadrature amplitude modulation (DP-16 QAM) system. Simulation results show that the superimposed TS has negligible negative effects on the transmission performance considering 7% forward error correction while the TO, FO, and rough CD estimation perform well after a long distance transmission. The max TO estimation (TOE) errors are, respectively, eight samples and 12 samples for QPSK and 16 QAM, and the max FO estimation errors are, respectively, 5.7 and 3.6 MHz for QPSK and 16 QAM. The rough CD estimation (CDE) error is below 946 ps/nm. The TOE and rough CDE separately decrease the complexity of frame synchronization and CDE. In total, the computation complexity of the estimations decreases by 91.8% compared to a regular blind estimation method.

Index Terms: Coherent optics communications, chromatic dispersion estimation, frequency offset estimation, frame synchronization, fractional Fourier transformation, training sequence

1. Introduction

With the development of cloud computation, everything connected and artificial intelligence, the data flow will keep the 22% compound annual growth rate in the future 5 years [1]. As the cornerstone of information society, optical fiber communication faces serious challenges and needs profound evolution. The future optical fiber network needs higher transmission rate, more flexible structure and lower cost. Digital signal processing (DSP) is an essential guarantee of signal recovery, especially in a long distance and high speed coherent optical communication systems.

Due to the characteristics of future flexible optical network, the accumulated chromatic dispersion (CD) from different fiber links, the frequency offset (FO) between local oscillator (LO) and carrier

laser source, and the timing offset (TO) due to the synchronization error vary from time to time. As a result, TO estimation (TOE), CD estimation (CDE) and FO estimation (FOE) are necessary and they have to be conducted at the very beginning in the DSP of receiver for the signal recovery. There have been many traditional methods to achieve the estimation in a single carrier system. For TOE, generally a known TS is inserted into the head of every frame. After CD compensation, one can calculate the correlation of the received signal and the TS point by point to find the frame head through the correlation peak position. For FOE, Fast Fourier transform based FOE (FFT-FOE) scheme is a periodogram method, where the maximization of the discrete-frequency spectrum of the fourth-power received samples can be acquired with the help of FFT [2]. For CDE, methods with a large estimation range usually rely on tentative cost function calculations by scanning CD value over a specific range [3], [4].

The above mentioned traditional estimation methods are performed separately with substantial computation complexity. Recently, novel estimation algorithms based on the Fractional Fourier transformation (FrFT) are proposed to achieve estimations simultaneously at a relatively low complexity [5]–[7]. As a generalized form of Fourier transformation (FT), FrFT is first proposed in [8]. Lohmann gives the geometry explanation [9] and Almeida explores the relationship between FrFT and traditional time-frequency tools from the view of DSP [10]. From then on, FrFT has been a powerful tool to deal with time-frequency problem in the communication system. In our previous arts [5], a joint TO and FO estimation is performed based on an FrFT TS, with strong robustness to optical signal-to-noise ratio (OSNR) degradation and large estimation range compared with [11], [12]. However, the FOE resolution in [5] is not precise enough and requires fractional FOE further. In addition, an FrFT based CDE method [6] has a stronger robustness to poor channel conditions and relatively lower computation complexity compared with [3] and [4]. However, it is still a CDE method by cost function scanning, in which every scan requires one time FrFT and auto-correlation. To our knowledge, the computational complexity of discrete FrFT is $N \times \log_2(N)$ at least [13]. Thus, the complexity is the biggest obstacle to applying the method to a real transmission system, still. In [14], a novel CDE method based on FrFT that does not require scanning CD is proposed, but it requires inserting two TS at 5 nm wavelength interval, which is unsuitable for a single carrier system.

In this paper, we design an FrFT tailored TS, which consists of 3 different FrFT TSs, to achieve 3 kinds of linear distortion estimation together: TOE, FOE and rough CDE. Different from our previous arts [5]–[7], the TS with extremely low power are superimposed directly on the transmitted signal and does not occupy additional time slot. Traditional TS always occupies the time slot and decreases the effective transmission rate, thereby decreasing the spectrum efficiency (SE). This is not the problem for our proposed method because our designed TS neither occupies the additional time slot, nor practically influences the transmission performance for its extremely low power. After specific FrFTs we can get 3 peaks from TS, by which TOE, FOE, CDE can be estimated at the same time. The feasibility of the proposed TS is verified by the simulation of 28 GBaud rate dual polarization quadrature phase-shift keying (DP-QPSK) and 16-ary quadrature amplitude modulation (DP-16 QAM) system. Thanks to the extremely low power of TS, the negative effect on the transmission performance is negligible considering the forward error correction (FEC) with 7% payload. For TOE, the max TOE errors are 8 samples for QPSK and 12 samples for 16 QAM. The correlation for synchronization only needs to be done around the peak found by TOE rather than the whole frame, thus decreasing the complexity of synchronization sharply. For FOE, the superimposed TS does not decrease SE and thus can be set longer to obtain more precise FOE. The max FOE errors are 5.7 MHz for QPSK and 3.6 MHz for 16 QAM, which does not require further fractional FOE anymore, compared to [5]. For CDE, rough CDE can be obtained without scanning the CD cost function and the rough CDE error is below 946 ps/nm. Similar to synchronization, the precise CDE in the latter only needs to scan around rough CDE rather than the whole CD range. All the estimation performances are accurate and stable in various transmission length and amplified spontaneous emission (ASE) noise. Compared to the regular estimation techniques, the total complexity of the proposed scheme decreases by 91.7% in total. By exploiting the superimposed TS, we can get a sharp decrease of computational complexity in the estimations, which does not require sacrificing the SE or other additional costs.

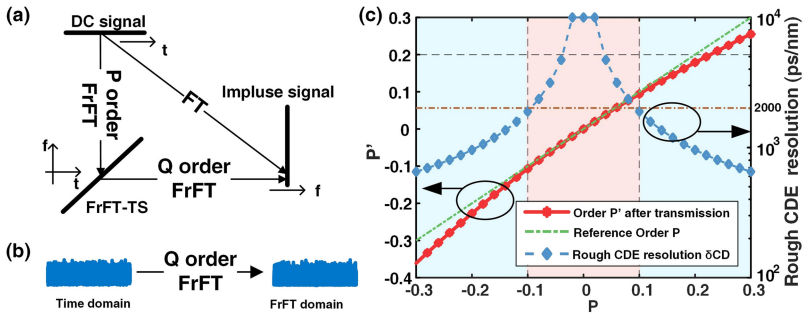

Fig. 1. (a) Decomposing one FT into two FrFT. (b) Transmitted signal after Q order FrFT. (c) P' and rough CDE error resolution versus P with CD.

2. Principle of Estimation

2.1 FrFT TS

The FrFT of a signal $f(t)$ with a rotation angle α, denoted as $F_\alpha(u)$, is defined in [8] as

$$F_\alpha(u) = \int_{-\infty}^{\infty} f(t) K_\alpha(t, u) dt \tag{1}$$

where the transform kernel $K_\alpha(t, u)$ of the FrFT is given by

$$K_\alpha(t, u) = \begin{cases} \sqrt{1 - j\cot(\alpha/2\pi)}\exp(j(t^2 + u^2)\cot(\alpha/2) - jtu/\sin\alpha) & \text{if } \alpha \text{ is not a multiple of } \pi \\ \delta(t - u) & \text{if } \alpha \text{ is a multiple of } 2\pi \\ \delta(t + u) & \text{if } \alpha + \pi \text{ is a multiple of } 2\pi \end{cases} \tag{2}$$

$$\alpha = P \times \frac{\pi}{2} \tag{3}$$

where P is the order of FrFT. When P is 1, FrFT will become FT. Operating a P order FrFT on the direct current (DC) signal, we can get a chirp signal named by FrFT TS, whose chirp parameter can be derived from the order P [9]. In time-frequency plane (Wigner plane), we can represent the FrFT TS by a slope line, which shows that the linear relationship between time and frequency of FrFT TS. The FrFT TS will converge into a peak of impulse signal in the middle position after a Q $(Q = 1-P)$ order FrFT. The process is equivalent to decomposing one FT into two FrFTs as shown in Fig. 1(a). In this paper, we superimpose the FrFT TS on the transmitted signal. After the Q order FrFT, the peak of FrFT TS can be distinguished among the transmitted signal, which serve as background noise in the FrFT domain as shown in Fig. 1(b).

Since we need to perform the linear distortions estimation at the very beginning of DSP before the CD compensation, the impact of CD to the FrFT TS must be considered. Due to the CD, different frequency components transmit at different speeds, which will change the order P to P'. P' can be obtained by finding the peak by scanning FrFTs of different orders on the received signal. The change mainly depends on the frequency range F covered by the FrFT TS:

$$F = Baud \times \sin\left(\frac{\pi}{2} \times |P|\right) \tag{4}$$

where $|P|$ denotes the absolute value of P and $Baud$ denotes the baud rate in the system.

As $|P|$ increases from 0 to 1, F will increase from 0 to the baud rate according to (4). To study CD impact on FrFT TSs of different orders, we simulate different orders P from -0.3 to 0.3 with 32000 ps/nm CD when the baud rate is 28 G. As shown in Fig. 1(c), the difference between P' and P decreases as $|P|$ decreases, and P' almost equals to P when $|P| \leq 0.1$. In this condition, the peak can be found by operating Q order FrFT on the received signal directly without considering the CD induced variation.

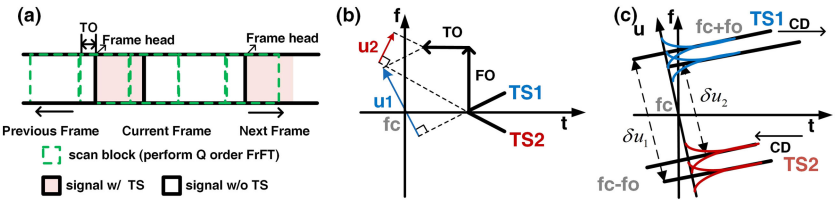

Fig. 2. (a) Find the rough place of FrFT TS. Principle of FrFT TS to estimate. (b) TO and FO. (c) CD.

2.2 TO, FO, and CD Estimation

FrFT TS with a length of *N* samples is superimposed over the head of every frame, and the first step of estimation is to find the rough place of FrFT TS. After transmission, we scan the received signals by performing a Q order FrFT block by block (one block contains *N* samples) as shown in Fig. 2(a). Due to TO, the block normally will not contain the integral FrFT TS, and the block of the highest peak after *Q* order FrFT covers the main part of FrFT TS. TO, FO and CD can be estimated with the specified block.

For the TOE and FOE, as shown in Fig. 2(b), two FrFT TSs with opposite orders *P* and *–P* named as TS1 and TS2 are overlapped in the time domain. After *Q* (1−P) and *–Q* (−1 + P) order FrFTs, we can get 2 peaks from TS1 and TS2, which should be at the middle position of the block in absence of TO and FO. However, TO and FO move the peaks along the time axis and frequency axis, respectively. In turn, the peak position shifts can be used to estimate TO and FO, which is illustrated detailedly in [5]. For TS1 and TS2, we define u_1 and u_2 as the peak shifts, which equals to the sample index of the peak minus *N/2* (half-length of one block). The *TO* measured in samples and *FO* measured in Hz are obtained as follows:

$$TOE = \frac{u_1 + u_2}{2 \times \sin(\pi Q/2)} \tag{5}$$

$$FOE = \frac{u_1 - u_2}{2 \times \cos(\pi Q/2)} \times df \tag{6}$$

where $df = Baud/N$. *df* and *N* denote minimum interval in the frequency domain and samples number of an FrFT TS, respectively.

For the CDE, as shown in Fig. 2(c), two identical FrFT TSs named as TS1 and TS2 are designed and overlapped in the time domain, but at different frequency *fc* ± *fo*, where *fc* is the central carrier frequency and *fo* is a preset FO. After transmission, the time delay $\Delta\tau$ between TS1 and TS2 is induced by CD:

$$\Delta\tau = (\lambda_1 - \lambda_2) \times CD \tag{7}$$

where $\lambda_1 = \frac{c}{fc - fo}$, $\lambda_2 = \frac{c}{fc + fo}$, *c* refers to the light speed.

The time delay can be estimated by the peaks shift. Due to the preset FO, the samples number between the peaks of TS1 and TS2 is δu_1, which changes to δu_2 after transmission. The orders of TS1 and TS2 are the same, so TO and FO induced by transmission move the peaks of TS1 and TS2 identically and make no contribution to δu_2. On the other hand, CD move the peaks of TS1 and TS2 in opposite directions along the time axis. Therefore, the change $\delta u_1 - \delta u_2$ only depends on the CD accumulation, which can be used to estimate the time delay $\Delta\tau$:

$$\Delta\tau = -\frac{\delta u_1 - \delta u_2}{\cos(\pi Q/2) \times N \times df} \tag{8}$$

Combining (7) with (8), the rough CDE equals to:

$$CDE_{rough} = -\frac{\Delta\tau}{(\lambda_1 - \lambda_2)} \tag{9}$$

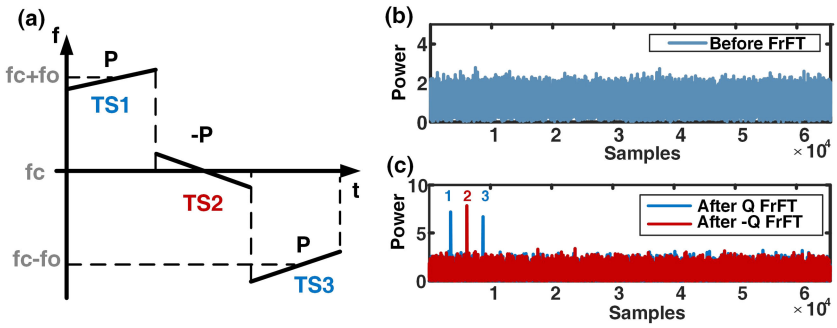

Fig. 3. (a) The proposed TS structure. The power of QPSK signal superimposed by FrFT TS (b) before FrFT (c) after FrFT.

In a single-carrier system, λ_1 and λ_2 are too close to get a precise CD. Thus precise CDE is performed next in the range of:

$$\left[\mathrm{CDE}_{rough}-\frac{1}{2}\delta\mathrm{CD}, \mathrm{CDE}_{rough}+\frac{1}{2}\delta\mathrm{CD}\right] \tag{10}$$

$$\delta CD = -\frac{1}{\cos(\pi Q/2)\times(\lambda_1-\lambda_2)\times N\times df} \tag{11}$$

where δCD refers to the rough CDE resolution for $\delta u_1 - \delta u_2 = 1$.

The obtained rough CDE can reduce the CD scanning times from $CD_{range}/\Delta CD$ to $\delta CD/\Delta CD$, where CD_{range} is the CD range in the optical network and CD scanning interval of precise CDE is ΔCD. Though the larger *fo* means smaller δCD, the *fo* is limited by the system bandwidth and thus cannot be set too large. In this paper, the simulation system bandwidth is set to 20 GHz. When *fc, fo* and baud rate are 193.12 THz, 7.5 GHz, and 28 GBaud respectively, we simulate the δCD versus *P* from −0.3 to 0.3 as shown in Fig. 1(c), where δCD larger than 10000 ps/nm is plotted as 10000 ps/nm for convenience. Because the rough CDE resolution δCD deteriorates when $|P|$ decreases, and in Section 2.1 we have found that the $|P|$ should be $\leq$0.1, thus we choose 0.1 as an optimal *P* value, where the δCD equals to 1834 ps/nm.

2.3 TS Structure and Superimposing Property

Based on the principle described above, we design a novel TS structure to estimate TO, FO and rough CD simultaneously before the CD compensation. As shown in the Fig. 3(a), the whole TS consists of 3 FrFT TSs named as TS1, TS2 and TS3, which are not overlapped in the time domain or the frequency domain. Every FrFT TS's length is *N* and the total length is $3\times N$, in which condition TO has the same effect on each FrFT TS. The orders of TS1 and TS3 are *P* and the order of TS2 is *–P*. The center frequency of TS1, TS2 and TS3 are separately set $fc+fo$, fc, $fc-fo$. TS1 and TS3 are identical TSs at different frequency, in charge of the rough CD estimation according to (9). Two groups of TS1 & TS2 and TS3 & TS2 have opposite orders, by which two groups of TOEs and FOEs can be obtained similar to [5]. In [5] the preset frequency of two opposite orders TS are both 0, so TOE and FOE should be revised due to preset FO compared with (5) and (6):

$$TOE_i = \frac{u_i + u_2 \pm fo/df \times \cos(\pi Q/2)}{2\times\sin(\pi Q/2)} \quad i = 1,3 \tag{12}$$

$$FOE_i = \frac{u_i - u_2 \pm fo/df \times \cos(\pi Q/2)}{2\times\cos(\pi Q/2)}\times df \quad i = 1,3 \tag{13}$$

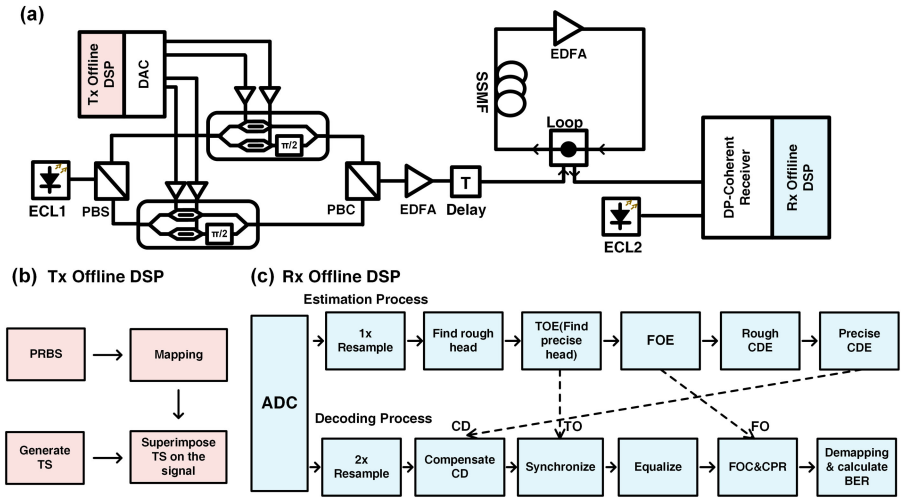

Fig. 4. (a) Simulation setup of the 28G DP-QPSK&16 QAM system, ECL: external cavity laser, DAC: analog-to-digital converter, PBS: polarization beam splitter, PBC: polarization beam combiner, SSMF: single mode fiber, EDFA: erbium doped fiber amplifier, ADC: analog-to-digital converter (b) Offline DSP in the transmitter. (c) Offline DSP in the receiver.

Where $\pm$ represents $-$ when $i = 1$; $\pm$ represents $+$ when $i = 3$. Due to preset offset, CD will influence TO between TS1 & TS2 and TS3 &TS2. Therefore, we average the two groups of TOEs and FOEs to remove the influence of CD on the TS1 and TS3.

It is worth noting that the TS is superimposed directly over the transmitted signal, rather than occupy additional time slot. It is explored on simulation whether the peak of superimposed FrFT TS is distinctive from the transmitted signal, which depends on TS power ratio and length. Here the power ratio of TS is defined by the ratio of average power of the TS to the transmitted signal measured in dB. In the time domain, the TS serves as the additive noise, so the power of TS should be set extremely low to ensure that TS will not harm the transmission performance. As has been mentioned in the Section 2.1, even though the power is extremely low, the distinguished peak of the TS can also be found after FrFT due to its convergence property. In Fig. 3(b), a length of 3×2^{12} TS with -21 dB power are superimposed at the beginning of a length of 2^{16} QPSK signals, whose signal to noise ratio is 5 dB. It is worth mentioning that the TS is just required in the beginning of a frame of signal for TOE for frame synchronization, and in this paper the frame length is set 2^{16} for convenience. Without FrFT operation, the TS power is so small that it is completely submerged in the QSPK signal. In Fig. 3(c), we find 2 peaks from TS1 and TS3 after a Q order FrFT (blue line), 1 peak from TS2 after a $-Q$ order FrFT (red line). These distinctive peaks promise an effective and stable estimation.

The estimation process is shown in Fig. 4(c): finding rough TS head is the first step, where for each polarization the received signals are scanned block by block (each block contains N samples) to find the peak after a Q order FrFT. If the first peak is observed at the *k-th* scan, the rough place will be: $TT = (k-1) \times N$. Starting from TT point, we extract $3 \times N$ samples and perform 2 times FrFT to obtain other two peaks. We average 2 *TOEs* from (12) using peak shifts u_1, u_2 and u_3, and the TS precise *head* is given by: $head = TOE + TT$. Again, we extract $3 \times N$ samples starting from *head* and perform 3 times FrFT to get the three peaks, which are used for the FOE and rough CDE. The repeat process can remove TO influence and improve the accuracy of FOE and CDE. We average 2 *FOEs* from (13) as the final FOE value. Then the rough CDE from (9) and precise CDE in [6] are followed. Our TOE method might have several samples error, so a known synchronization TS is inserted to locate the frame head by correlation point by point. It is an additional traditional TS placed at the beginning of the signal frame to ensure an absolutely accurate frame synchronization with no error. The correlation peak can be found near TS precise *head* rather than the whole signal, which sharply decreases the calculation complexity of synchronization.

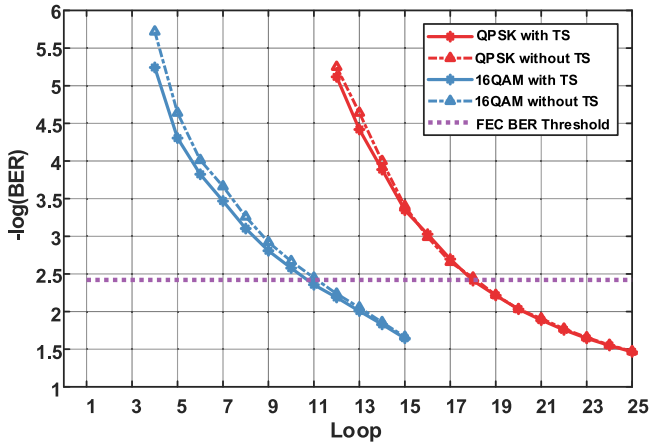

Fig. 5. QPSK and 16 QAM BER performance for different loops.

3. Results and Discussions

The feasibility of the proposed method is verified by the simulation using VPItransmissionMaker Optical System 9.8 and MATLAB, and the simulation setup is shown in Fig. 4(a). QPSK or 16 QAM signals with a length of 2^{16}, superimposed with our proposed TS are generated from pseudo-random bit sequence (PRBS) in the Tx offline DSP as shown in Fig. 4(b), which contain synchronization TS with a length of 128. Then DAC and electrical drivers provide electrical signals to DP-I/Q modulator at 56G Sam/s. Meanwhile, the ECL1 with 100-KHz linewidth serves as an optical source. Then optical signals are amplified to 0 dBm, delayed by the signal delay module and sent to the fiber loop. The loop contains 100-km SSMF and an ideal EDFA, fully compensating fiber loss with 5 dB noise figure. The CD parameter of SSMF is 16 ps/(nm $\times$ km) and one loop accumulates 1600 ps/nm CD. In order to simulate various linear distortion conditions, we set TOs by changing the value of delay time in signal delay module, FOs by setting the frequency of local oscillator ECL2 different from carrier laser source ECL1, and CDs by setting the loop number. TOs range from –1/2 to 1/2 of one FrFT TS length, FOs range from –5 GHz to +5 GHz, and CDs range from 1600 ps/nm to 40000 ps/nm. After the loop transmission, the signals are received by a DP-coherent receiver with 20 GHz bandwidth and processed in Rx offline DSP. As shown in Fig. 4(c), the data are sampled by the analog-to-digital converter and sent to DSP offline. The estimation process includes 1-time symbol rate resampling, finding rough head, TOE, FOE, rough and precise CDE. The dashed arrows in Fig. 4(c) indicate that the TO, FO and CD estimation results provide channel information for the corresponding decoding process. The decoding process includes 2-time symbol rate resampling, CD compensation (overlap frequency domain CD compensation [15]), synchronization, equalization (constant modulus algorithm (CMA) for QPSK [16] and CMA radius directed equalization [17] for 16 QAM), FO compensation, phase recovery (Viterbi-Viterbi for QPSK [18] and QPSK partition [19] for 16 QAM), constellation demapping and BER calculation. It is worth mentioning that in the decoding process, the superimposed TS just acts as the tiny additive noise, so the decoding algorithms used are exactly the same as the traditional ones.

First, to minimize the negative effects of superimposed TS on the transmission and ensure the distinguishable peak of the TS, we adjust the TS power and length according to the modulation format used. Because 16 QAM signals are less resistant to distortion than QPSK signals, the power of superimposed TS for 16 QAM is less than that for QPSK. We finally choose TS with a length of 3×2^{12} and -18 dB power ratio for QPSK, and TS with a length of 3×2^{13} and -27 dB power ratio for 16 QAM. The relationships between BER and loop number for QPSK and 16 QAM are shown in Fig. 5. The BER performances of QPSK and 16 QAM without TS are obtained with traditional estimation methods in [2], [6]. The estimation result of our proposed scheme and traditional scheme is identical, so the tiny BER performance difference only comes from the superimposed TS. The

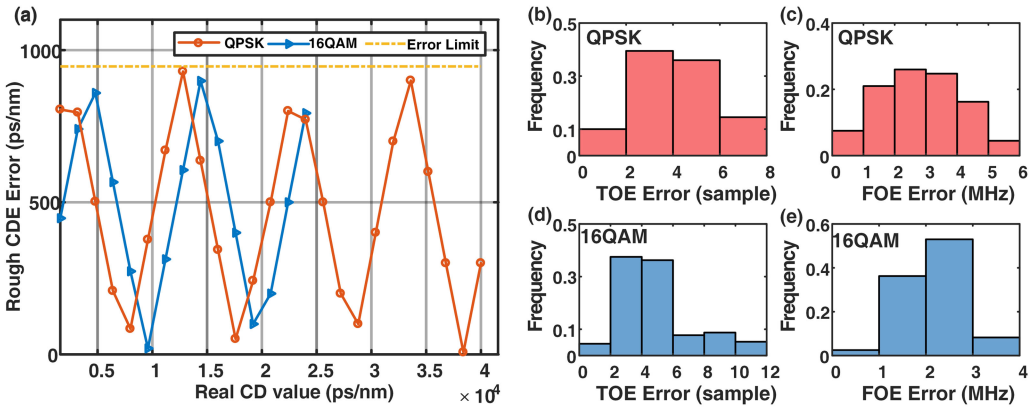

Fig. 6. (a) QPSK and 16 QAM rough CDE error. (b)−(e) TOE and FOE error histogram for QPSK and 16 QAM.

superimposed TS acts as the additive noise in the time domain, so the BER performance is slightly worse than the signal without TS. It can be noted that the BER difference between signal with and without TS decreases as the transmission loop increases. This is because the noise from the EDFA accumulates and dominates, and hence the effect of superimposed TS can be neglected. Considering the FEC with 7% overhead, the longest effective transmission length of the schemes with TS is the same as the schemes without TS at BER threshold of 3.8×10^{-3}. When BER is less than the FEC threshold, the signal can be identified with no error. Thus, our proposed method does not sacrifice the SE because the TSs do not occupy additional time slot or degrade transmission performance with 7% FEC for QPSK and 16 QAM signals, respectively.

Second, we test the rough CDE performance with various transmission length as shown in Fig. 6(a). As the loop number increases, the ASE noise and the BER increase. We separately limit the max transmission length to 2500 km and 1500 km for QPSK and 16 QAM, where BERs are as high as 0.02 and 0.03. For different loops, the rough CDE errors of QPSK and 16 QAM are below the rough CDE error limit, which is half of δCD, 946 ps/nm. The result shows that CDE method performs well in various CD values and has a strong robustness to ASE noise. In addition, one loop accumulates 1600 ps/nm CD, which is different from δCD, so the rough CDE errors change with real CD periodically. After that, the blind CDE in [6] will be performed around the rough CDE to obtain the precise CD estimation result.

Next, we test TOE and FOE by separately setting 400 different TO and FO values. The histograms of TOE and FOE errors for QPSK and 16 QAM are separately showed in the Fig. 6 (b)–(e). The mean TOE errors of QPSK and 16 QAM are 4.1 samples and 4.3 samples, and the mean FOE errors of QPSK and 16 QAM are 2.8 MHz and 2.1 MHz, respectively. Considering the worst condition, the max TOE errors of QPSK and 16 QAM are respectively 8 samples and 12 samples. The max FOE errors of QPSK and 16 QAM are 5.7 MHz and 3.6 MHz. For TOE, there still exist several sample errors, so an additional traditional TS mentioned in Section 2.3 is utilized to ensure an absolute accurate synchronization by correlation method. For FOE, the result satisfies the requirements in the practical application and does not require further FOE any more.

Specifically, we compare the computation complexity of TOE, FOE and CDE between the proposed estimation method and regular estimation method. Because the samples number vary in different methods, we count the total number of multiplies and only the major complexity part of each method is counted for convenience. The unit of computational complexity is per symbol for all the estimation methods below. The regular estimation methods are listed as follows: for TOE, synchronization is performed by cross-correlation (O(n)) of a known TS with a length of 128. We assume that the length of a frame is 2^{16}, so the cross-correlation is performed 2^{16} times in total. For FOE, to reach the same accuracy as our method, FFT-FOE requires 1024 samples to perform FFT ($O(n \times \log_2(n))$). For CDE, we assume that CDE range and the max CDE error are separately

TABLE 1
Computation Complexity Analysis

Estimation Process \ Estimation Method		The proposed method	The regular method [2,6]
Find rough place		$2^{16}/2^{12}$=16 times FrFT (2^{12})	none
TOE		2+3=5 times FrFT (2^{12})	none
FOE			1 time FFT (2^{10})
Rough CDE			none
Precise CDE		1892/200+1=10 times FrFT (2^{12}) and auto-correlation (2^{12})	40000/200+1=201 times FrFT (2^{12}) and auto-correlation (2^{12})
Synchronization		2×8+1=17 times cross-correlation (2^7)	65535 times cross-correlation (2^7)
Each Process Multiplies	1 time FrFT	$2^{12}\times\log_2(2^{12})$ = 49152 multiplies	
	1 time auto-correlation	2^{12}=4096 multiplies	
	1 time FFT	$2^9\times\log_2(2^9)$ = 4068 multiplies	
	1 time cross-correlation	2^7=128 multiplies	
Total multiplies		(16+5)×49152+10×(4096+49152)+17×128= 1566848 multiplies	1024×10+201×(49152+4096)+65536×128= 19101696 multiplies

40000 ps/nm and 200 ps/nm, where CD scanning is performed $40000/200 + 1 = 201$ times and the residual CD can be compensated in the latter equalization process [17], [18]. To satisfy the demand, the precise CDE method [8] requires 4096 samples to perform FrFT ($O(n \times \log_2(n))$) and auto-correlation ($O(n)$). It has been illustrated in [6] that the computational complexity of FrFT based CDE is less than that of the other CDE methods such as time domain method and frequency domain method in [3], [4]. The proposed estimation method is analyzed when the length of TS is 3×2^{12}. Finding rough head requires $2^{16}/2^{12} = 16$ times FrFT, and TOE, FOE and CDE require 5 times FrFT as mentioned in Section 2.3. The max TOE error is 8 samples, so synchronization requires additional $8 \times 2 + 1 = 17$ times cross-correlation. The rough CDE resolution is 1832 ps/nm and the precise CDE requires $1832/200 + 1 = 10$ times CD scanning, where the decimal part is omitted. The specific processes, the samples number (in parenthesis) and the multiplies of each process are completely listed in Table 1. The main contribution of decreasing complexity comes from synchronization and CDE. The total multiplies of the proposed method and the regular method are respectively 1566848 and 19101696, leading to a 91.8% complexity decrease in total. It is a really sharp decrease and provides a low-latency and low power consumption scheme for the elastic coherent receiver.

4. Conclusion

In this paper, we design an FrFT tailored TS to simultaneously estimate the linear distortions: TO, FO and rough CD for coherent optical communication. The TS with extremely low power is superimposed directly on the transmitted signal and does not decrease the SE. Based on the simulation results, the superimposed TS will also not impact on the transmission performance practically with 7% FEC. The estimation results are stable for various transmission length. For FOE, the max error is separately 5.7 MHz for QPSK and 3.2 MHz for 16 QAM, which satisfy the accuracy need. For TOE and CDE, we can get a rough CDE and TOE with several samples error, by which the complexity of CDE and frame synchronization can be sharply decreased. Under the condition of 40000 ps/nm CD and 2^{16} frame length, the computational complexity is decreased by 91.8% totally, which provides a low-latency and low power consumption scheme for elastic coherent receiver.

References

[1] Cisco VNI, "The zettabyte era: Trends and analysis," Cisco, San Jose, CA, USA, *White Paper*, 2016.
[2] M. Selmi, Y. Jaouën, P. Ciblat, and B. Lankl, "Accurate digital frequency offset estimator for coherent PolMuxm QAM transmission systems," in *Proc. Eur. Conf. Opt. Commun.*, Sep. 2009, Paper P3.08.
[3] M. Kuschnerov, M. Kuschnerov, F. N. Hauske, and K. Piyawanno, "DSP for coherent single-carrier receivers," *J. Lightw. Technol.*, vol. 27, no. 16, pp. 3614–3622, Aug. 2009.
[4] F. N. Hauske, Z. Zhang, C. Li, C. Xie, and Q. Xiong, "Precise, robust and least complexity CD estimation," in *Proc. Int. Conf. Opt. Fiber Commun.*, San Diego, CA, USA, Mar. 2011, Paper JWA032.
[5] H. Zhou *et al.*, "Joint timing/frequency offset estimation and correction based on FrFT encoded training symbols for PDM CO-OFDM systems," *Opt. Exp.*, vol. 24, no. 25, pp. 28256–28269, Dec. 2016.
[6] H. Zhou *et al.*, "Fractional fourier transformation-based blind chromatic dispersion estimation for coherent optical communications," *J. Lightw. Technol.*, vol. 34, no. 10, pp. 2371–2380, May 2016.
[7] H. Zhou *et al.*, "Joint estimation of time-frequency impairments for single carrier coherent transmission system with FrFT tailored training symbol," in *Proc. Int. Conf. Opt. Fiber Commun.*, San Diego, CA, USA, Mar. 2017, Paper W2A.58.
[8] V. Namias, "The fractional order Fourier transform and its application to quantum mechanics," *IMA J. Appl. Math.*, vol. 25, pp. 241–265, Mar. 1980.
[9] A. W. Lohmann, "Image rotation, Wigner rotation, and the fractional Fourier transform," *J. Opt. Soc. Amer. A*, vol. 10, no. 10, pp. 2181–2186, Nov. 1993.
[10] L. B. Almeida, "The fractional Fourier transform and time-frequency representations," *IEEE Trans. Signal Process.*, vol. 42, no. 11, pp. 3084–3091, Nov. 1994.
[11] X. Yi, W. Shieh, and Y. Ma, "Phase noise effects on high spectral efficiency coherent optical OFDM transmission," *J. Lightw. Technol.*, vol. 26, no. 10, pp. 1309–1316, Jun. 2008.
[12] S. L. Jansen, I. Morita, T. C. W. Schenk, N. Takeda, and H. Tanaka, "Coherent optical 25.8-Gb/s OFDM transmission over 4160-km SSMF," *J. Lightw. Technol.*, vol. 26, no. 1, pp. 6–15, Feb. 2008.
[13] H. M. Ozaktas, O. Arikan, M. A. Kutay, and G. Bozdagt, "Digital computation of the fractional Fourier transform," *IEEE Trans. Signal Process.*, vol. 44, no. 9, pp. 2141–2150, Sep. 1996.
[14] W. Wang, Y. Qiao, A. Yang, and P. Guo, "A novel noise-insensitive chromatic dispersion estimation method based on fractional Fourier transform of LFM signals," *IEEE Photon. J.*, vol. 9, no. 1, Feb. 2017, Art. no. 7100312.
[15] R. Kudo *et al.*, "Coherent optical single carrier transmission using overlap frequency domain equalization for long-haul optical systems," *J. Lightw. Technol.*, vol. 27, no. 16, pp. 3721–3728, Aug. 2009.
[16] D. S. Millar and S. J. Savory, "Blind adaptive equalization of polarization-switched QPSK modulation," *Opt. Exp.*, vol. 19, no. 9, pp. 8533–8538, Apr. 2011.
[17] X. Xu, B. Châtelain, and D. V. Plant, "Decision directed least radius distance algorithm for blind equalization in a dual-polarization 16-QAM System," in *Proc. Int. Conf. Opt. Fiber Commun.*, Los Angeles, CA, USA, Mar. 2012, Paper OM2H.5.
[18] A. J. Viterbi and A. M. Viterbi, "Nonlinear estimation of PSK-modulated carrier phase with application to burst digital transmission," *IEEE Trans. Inf. Theory*, vol. 29, no. 4, pp. 543–551, Jul. 1983.
[19] I. Fatadin, D. Ives, and S. J. Savory, "Blind equalization and carrier phase recovery in a 16-QAM optical coherent system," *J. Lightw. Technol.*, vol. 27, no. 15, pp. 3042–3049, May 2009.